SURE-LET Image Denoising with Directional LOTs

Shogo MURAMATSU, Dandan HAN and Hisakazu KIKUCHI
Niigata University, 8050 2-no-cho, Ikarashi, Nishi-ku, 950-2181, Niigata, Japan
E-mail: shogo@eng.niigata-u.ac.jp Tel: +81-25-262-6746

***Abstract*—This paper proposes to adopt hierarchical tree construction of directional lapped orthogonal transforms (DirLOTs) to image denoising. The DirLOTs are 2-D non-separable lapped orthogonal transforms with directional characteristics. The bases are allowed to be anisotropic with the fixed-critically-subsampling, overlapping, orthogonal, symmetric, real-valued and compact-support property. As well, it is possible to introduce the trend vanishing moments (TVMs), which force wavelet filters to annihilate trend surface components. So far, the orthonormal wavelet image denoising techniques, such as the SURE-LET approach by Luisier *et al.*, have shown a disadvantage in the restoration of diagonal textures and edges because of the separability of the adopted transforms. This work shows through some experimental results that the SURE-LET approach with DirLOTs overcomes the geometric problem.**

I. Introduction

Denoising is one of the most important image processing applications since images are usually corrupted with additive noise through image acquisition and transmission. The noise is often modeled as white Gaussian. This statistical hypothesis or prior knowledge on noise gives us several denoising algorithms which preserve features of the noiseless clean images. For a couple of decades, such denoising algorithms have been developed with sparse representation of images, which includes orthonormal wavelets [1]. One of the most popular techniques is the soft-thresholding introduced by Donoho and Johnstone [2], [3]. In the article [3], the authors proposed to minimize Stein's unbiased risk estimator (SURE) for determining the shape of shrinkage function and used it in the wavelet domain. The SURE approach has an advantage that no statistical prior knowledge on the clean unknown image is required, while Bayesian approaches requires the knowledge of the pdf. This fact makes the procedure simple, while keeping the efficiency.

The shrinkage function, however, is piece-wise linear and governed by a single threshold parameter T. Thus, the shape is strongly restricted and the relation between the shape and threshold is not linear. As a result, finding an optimal threshold T requires nonlinear search algorithm. In order to relax the restriction, Lusier *et al.* proposed a linearly parameterized denoising function so that the optimal solution search becomes linear [4]–[6]. The technique is referred to as the SURE-LET (linear expansion of thresholds) approach and can be used for interscale orthonormal wavelet shrinkage.

The SURE-LET thresholding is efficient both in terms of computational complexity and denoising quality. However, the quality becomes lower for regions where the interscale correlation is weak. Conventionally, orthonormal wavelet thresholding adopts separable transforms such as Haar transform and Symlets. Such separable transforms have disadvantage in representing diagonal edges, textures and gradually changing content, where the transform coefficients are scattered around several high-frequency subbands. Consequently, the sparse representation fails.

Recent development of image transforms involves non-separable transforms for handling such diagonal structures [7]–[12]. The curvelet is one of the successful 2-D transforms, which can efficiently approximate smooth curve edges [8], [9]. It, however, is overcomplete and initially developed in continuous domain, and constructing a fast discretized orthogonal curvelet-like transform is an open problem. In the article [11], Do and Vetterli start with discrete-domain construction of filter banks for producing an alternative directional multiresolution analysis framework. The transform, however, is non-orthogonal [11], [12].

Orthonormal transforms are preferable for many applications since they preserve the energy between a given original signal and the transform coefficients, and reduce mathematical handling of algorithms significantly. The non-redundancy is also attractive for the application to compression. As a previous work, we have proposed 2-D directional lapped orthogonal transforms (DirLOTs) [13]–[16]. The bases are allowed to be anisotropic with the fixed-critically-subsampling, overlapping, orthogonal, symmetric, real-valued and compact-support property. As well, it is possible to give the trend vanishing moments (TVMs), which force wavelet filters to annihilate trend surface components. This paper proposes to adopt the hierarchical tree construction of the DirLOTs, i.e. 2-D non-separable orthonormal symmetric DWTs, to the SURE-LET denoising so that the denoising quality for diagonal textures and edges is improved. It is worth noting that the group delay compensation (GDC) filter is simply obtained since each basis image is symmetric or anti-symmetric and has the same center of symmetry.

The organization of this paper is as follows: In Section II, as a preliminary, the SURE-LET image denoising is briefly reviewed. Then, Section III introduces the DirLOTs and shows some of the design examples. In Section IV, some experimental results of the SURE-LET image denoising with the DirLOTs are shown, followed by the conclusion in Section V.

II. Review of SURE-LET Image Denoising

In this section, let us review the SURE-LET approach of image denoising, We here note that the symbol $\mathbf{I}$ is reserved for denoting the identity matrix.

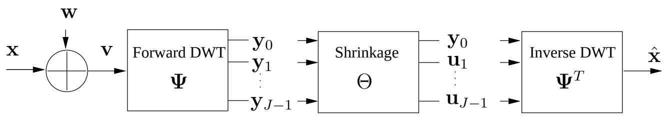

Fig. 1. Principle of orthonormal wavelet denoising

A. Problem Setting

Image acquisition devices provide pixels $\mathbf{v} = \begin{pmatrix} v_0 & v_1 & \cdots v_{N-1} \end{pmatrix}^T$, where N denotes the number of pixels. The observed picture $\mathbf{v}$ is usually corrupted with noise $\mathbf{w}$ and the noise $\mathbf{w}$ is frequently modeled as an additive white Gaussian noise (AWGN) with zero mean and no correlation to the other pixels. Let $\mathbf{x}$ be the original clean noiseless picture. Then, the observed image $\mathbf{v}$ is represented by

$$\mathbf{v} = \mathbf{x} + \mathbf{w},$$

where $E\{\mathbf{w}\} = 0$ and $E\{\mathbf{w}\mathbf{w}^T\} = \sigma^2\mathbf{I}$.

Image denoising in this study deals with the problem of finding a good candidate $\hat{\mathbf{x}}$ of unknown noiseless picture $\mathbf{x}$ only from the observed picture $\mathbf{v}$. The estimation process can be represented by the following formulation:

$$\hat{\mathbf{x}} = \mathbf{F}(\mathbf{v}),$$

where $\mathbf{F}$ is a denoising function.

Figure 1 shows the principal of orthonormal wavelet denoising, where $\boldsymbol{\Psi}$, Θ and $\boldsymbol{\Psi}^T$ are a forward discrete wavelet transform (DWT), a shrinkage function and the inverse DWT. The symbol $\mathbf{y}_j$ denotes the j-th subimage, where $\mathbf{y}_0$ consists of scaling coefficients and $\mathbf{y}_j$ for $j \in [1, J-1]$ possess wavelet coefficients, while $\mathbf{u}_j$ for $j \in [1, J-1]$ denote the denoised wavelet coefficients through shrinkage operation Θ. The wavelet denoising process is summarized as follows:

i) Perform a forward DWT of the noisy picture $\mathbf{v} = \mathbf{x} + \mathbf{w}$. Then, obtain the transform coefficients

$$\mathbf{y} = \begin{pmatrix} \mathbf{y}_0^T & \mathbf{y}_1^T & \cdots & \mathbf{y}_{J-1}^T \end{pmatrix}^T = \boldsymbol{\Psi}\mathbf{v}.$$

ii) Denoise wavelet subimages $\mathbf{y}_j$ for $j \in [1, J-1]$. Then, obtain denoised subimages

$$\mathbf{u} = \begin{pmatrix} \mathbf{y}_0^T & \mathbf{u}_1^T & \cdots & \mathbf{u}_{J-1}^T \end{pmatrix}^T = \Theta(\mathbf{y}).$$

iii) Perform the inverse DWT of coefficients $\mathbf{u}$ as

$$\hat{\mathbf{x}} = \boldsymbol{\Psi}^{-1}\mathbf{u} = \boldsymbol{\Psi}^T\mathbf{u}.$$

In this framework, the denoising function $\mathbf{F}$ is represented by

$$\mathbf{F}(\mathbf{v}) = \boldsymbol{\Psi}^T\Theta(\boldsymbol{\Psi}\mathbf{v}). \quad (1)$$

Note that the denoising quality depends on the choice of the transform $\boldsymbol{\Psi}$ and the shrinkage function Θ.

B. SURE-LET Approach

The SURE-LET approach is a technique to realize the shrinkage function Θ, which avoids any a priori hypotheses on the noiseless picture $\mathbf{x}$ under the usual white Gaussian noise assumption. The denoising problem is reformulated as the search for the denoising process that minimizes the Stein's unbiased risk estimate (SURE). The denoising process is completely characterized by a set of parameters. In the article [4], Luisier *et al.* proposed the following point-wise thresholding

$$\theta(y) = \sum_{k=1}^{K} a_k y e^{-(k-1)\frac{y^2}{2T^2}},$$

where y is a wavelet coefficient. In this function, the authors suggested to use $K = 2$ and $T = \sqrt{6}\sigma$.

Furthermore, the authors also proposed the following form of the shrinkage function:

$$\theta(y, y_p; \mathbf{a}, \mathbf{b}) = e^{-\frac{y_p^2}{12\sigma^2}} \sum_{k=1}^{K} a_k y e^{-(k-1)\frac{y^2}{12\sigma^2}} + \left(1 - e^{-\frac{y_p^2}{12\sigma^2}}\right) \sum_{k=1}^{K} b_k y e^{-(k-1)\frac{y^2}{12\sigma^2}}, \quad (2)$$

where y_p is an interscale prediction of y obtained from the wavelet parent-child relationship. This predictor tells us only an indication on its expected magnitude. Thus, the authors use the parent y_p as a discriminator between high and low SNR wavelet coefficients. Consequently, the parameters a_k and b_k are linearly solved for minimizing SURE.

III. Image Denoising with Directional LOT

The wavelet denoising function $\mathbf{F}$ in Eq (1) is governed by the choice of DWT $\boldsymbol{\Psi}$ as well as the shrinkage function Θ. In this section, we propose to use the directional LOT as a critically sampled orthonormal wavelet basis $\boldsymbol{\Psi}$.

In the followings, the decimation matrix is fixed to 2×2 in order to construct 2-D DWT trees. We reserve the symbol $\mathbf{E}_0$ to the 4×4 symmetric orthonormal transform given directly through the 2-D separable DCT, where each basis image is aligned into an 4×1 vector and is arrayed into the form $\mathbf{E}_0^T = \begin{pmatrix} \mathbf{b}_{\mathrm{ee}} & \mathbf{b}_{\mathrm{oo}} & \mathbf{b}_{\mathrm{oe}} & \mathbf{b}_{\mathrm{eo}} \end{pmatrix}$, where $\mathbf{b}_{\mathrm{ee}}$, $\mathbf{b}_{\mathrm{oo}}$, $\mathbf{b}_{\mathrm{oe}}$ and $\mathbf{b}_{\mathrm{eo}}$ are 4×1 vectors consisting of columnized basis images. The first and second subscript denote the symmetry in the vertical and horizontal direction, where 'e' and 'o' describe even- and odd-symmetry, respectively. The symbols $\mathbf{O}_m$ and $\mathbf{I}_m$ are reserved for the $m \times m$ null and identity matrix, respectively. A product of sequential matrices is denoted by $\prod_{n=1}^{N} \mathbf{A}_n = \mathbf{A}_N \mathbf{A}_{N-1} \cdots \mathbf{A}_2 \mathbf{A}_1$.

A. Lattice Structure of 2-D Non-separable LOTs

In the articles [13]–[16], we have shown a method to construct 2-D nonseparable LOTs with a lattice structure. Figure 2 illustrates the structure, where $\mathbf{d}(\mathbf{z})$ is defined as a 2-D delay chain of size 4×1 by $[\mathbf{d}(\mathbf{z})]_\ell = z_{\mathrm{y}}^{-((\ell))_{M_{\mathrm{y}}}} \cdot z_{\mathrm{x}}^{-\lfloor \ell / M_{\mathrm{y}} \rfloor}$, where $\mathbf{z} = (z_{\mathrm{y}}, z_{\mathrm{x}})^T \in \mathcal{C}^2$, $((x))_M$ and $\lfloor x \rfloor$ denote the

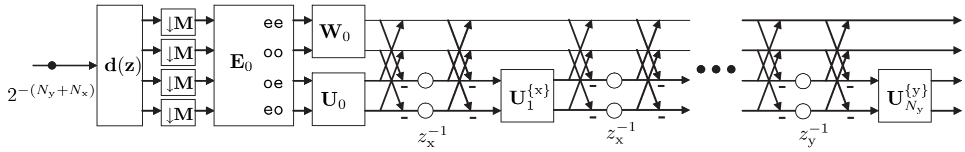

Fig. 2. Lattice structure of a 2-D non-separable GenLOT (forward transform).

modulo x of M and the largest integer less than or equal to x, respectively. The corresponding polyphase matrix of order $[N_\mathrm{y}, N_\mathrm{x}]$ is represented by the following product form:

$$\mathbf{E}(\mathbf{z}) = \prod_{n_\mathrm{y}=1}^{N_\mathrm{y}} \left\{ \mathbf{R}_{n_\mathrm{y}}^{\{y\}} \mathbf{Q}(z_\mathrm{y}) \right\} \cdot \prod_{n_\mathrm{x}=1}^{N_\mathrm{x}} \left\{ \mathbf{R}_{n_\mathrm{x}}^{\{x\}} \mathbf{Q}(z_\mathrm{x}) \right\} \cdot \mathbf{R}_0 \mathbf{E}_0, \tag{3}$$

where $\mathbf{Q}(z_d) = \frac{1}{2}\begin{pmatrix} \mathbf{I}_2 & \mathbf{I}_2 \\ \mathbf{I}_2 & -\mathbf{I}_2 \end{pmatrix}\begin{pmatrix} \mathbf{I}_2 & \mathbf{O}_2 \\ \mathbf{O}_2 & z_d^{-1}\mathbf{I}_2 \end{pmatrix}\begin{pmatrix} \mathbf{I}_2 & \mathbf{I}_2 \\ \mathbf{I}_2 & -\mathbf{I}_2 \end{pmatrix}$, $\mathbf{R}_0 = \begin{pmatrix} \mathbf{W}_0 & \mathbf{O}_2 \\ \mathbf{O}_2 & \mathbf{U}_0 \end{pmatrix}$, $\mathbf{R}_n^{\{d\}} = \begin{pmatrix} \mathbf{I}_2 & \mathbf{O}_2 \\ \mathbf{O}_2 & \mathbf{U}_n^{\{d\}} \end{pmatrix}$. Symbols $\mathbf{W}_0$, $\mathbf{U}_0$ and $\mathbf{U}_{n_\mathrm{d}}^{\{d\}}$ denote orthonormal matrices of size 2×2 and freely controlled during the design process. Equation (3) guarantees the orthonormality and symmetry. The support region of each analysis (or synthesis) filter results in $L_\mathrm{y} \times L_\mathrm{x} = 2(N_\mathrm{y} + 1) \times 2(N_\mathrm{x} + 1)$.

B. TVM Condition

The 2-D non-separable LOTs can be constructed under the trend vanishing moment (TVM) constraints so that a proper directional characteristic is provided. The TVM condition is defined as follows, where we refer to $H_0(\mathbf{z})$ as a scaling filter and $H_k(\mathbf{z})$ for $k \geq 1$ as a wavelet filter.

Definition 1 (Trend Vanishing Moments of Order P). *We say that a filter bank has P-order TVM along the direction $\mathbf{u}_\phi = (\sin\phi, \cos\phi)^T$ if trend moments $\mu_{k,\phi}^{(p)}$ of all wavelet filters up to $p = (P-1)$ vanishes, i.e.*

$$0 = \mu_{k,\phi}^{(p)} = \sum_{\mathbf{n}\in\mathcal{Z}^2} h_k[\mathbf{n}] \sum_{q=0}^{p} \binom{p}{q} (n_\mathrm{y}\sin\phi)^{p-q}(n_\mathrm{x}\cos\phi)^q \tag{4}$$

for all $k = 1, 2, \cdots, M-1$ and $p = 0, 1, \cdots, P-1$, where $\mathbf{n} = [n_\mathrm{y}, n_\mathrm{x}]^T$ and $h_k[\mathbf{n}]$ is the impulse response of the k-th analysis filter.

The one-order TVM is identical to the classical one-order VM and guarantees the no-DC-leakage property. As well, the wavelet filters with the two-order TVMs annihilate piecewise one-order trend surfaces in the direction $\mathbf{u}_\phi$, i.e. functions proportional to $(n_\mathrm{y}\sin\phi + n_\mathrm{x}\cos\phi)$. Figure 3 shows a design example of a DirLOT with the two-order TVMs. The directional property works well for diagonal textures and edges.

IV. Experimental Results

This section shows some experimental results of the wavelet denoising with the SURE-LET approach in order to verify the significance of the proposed construction, i.e. the combination of the SURE-LET approach as the shrinkage function and a hierarchical DirLOT as the orthonormal DWT. In this experiments, as was suggested in the article [4], the interscale shrinkage function given in Eq. (2) was adopted, where the parameters K and T are selected as $K = 2$ and $T = \sqrt{6}\sigma$. We adopt the DirLOT shown in Fig. 5, which was designed by the procedure given in the article [16].

Figures 4 and 5 show the experimental results. In this experiments, 8-bit grayscale textures of size 128×128 pixels were used, where the noise level was set to $\sigma = 30$. The

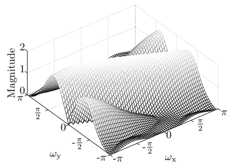

(a) $|H_0(e^{j\boldsymbol{\omega}^T})|$

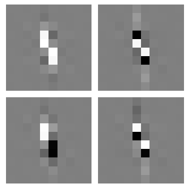

(b) Basis images

Fig. 3. A design example with the two-order TVMs of $\phi = \cot^{-1}\alpha = \cot^{-1}(-2.0) \sim -0.4636$[rad], where $[N_\mathrm{y}, N_\mathrm{x}]^T = [4,4]^T$, i.e. the basis images are of size 10×10.

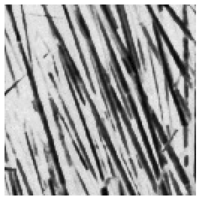

(a) Original

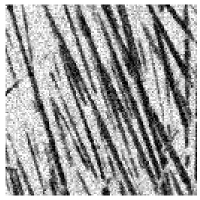

(b) Noisy picture

(c) Sym5

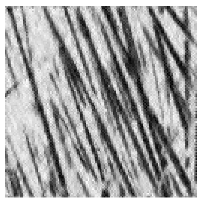

(d) VM2

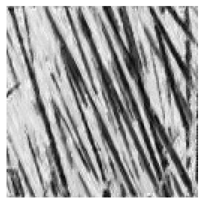

(e) TVM

Fig. 4. Denoising results, for an 8-bit grayscale picture of size 128×128 pixels. (a)Original picture, (b)Noisy picture with white Gaussian ($\sigma = 30$). (c),(d) and (e) are denoised results, where Sym5, VM2 and TVM denote Symlets of index 5, DirLOT with the classical VM of order two and DirLOT with the two-order TVMs, respectively. The number of hierarchical levels is three.

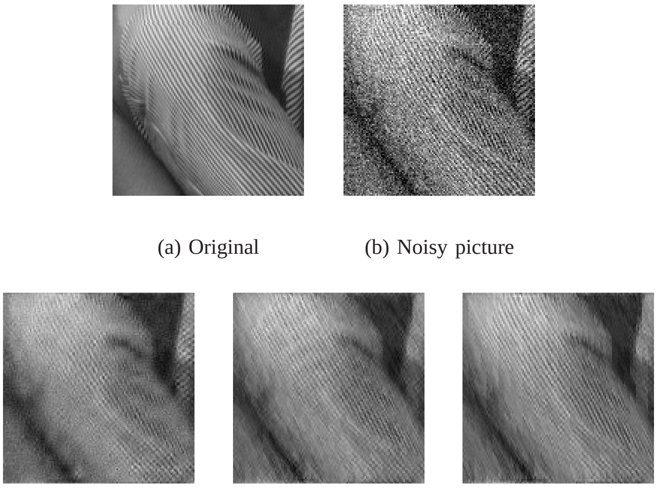

(a) Original (b) Noisy picture

(c) Sym5 (d) VM2 (e) TVM

Fig. 5. Denoising results, for an 8-bit grayscale picture of size 128×128 pixels. (a)Original picture, (b)Noisy picture with white Gaussian ($\sigma = 30$). (c),(d) and (e) are denoised results, where Sym5, VM2 and TVM denote Symlets of index 5, DirLOT with the classical VM of order two and DirLOT with the two-order TVMs, respectively. The number of hierarchical levels is three.

TABLE I
COMPARISON OF PSNRS AND SSIM INDEXES AMONG THREE TRANSFORMS FOR VARIOUS NOISE LEVELS.

	Sym5	VM2	TVM	Sym5	VM2	TVM
Fig. 4	PSNR			SSIM		
$\sigma = 10$	**29.47**	23.97	28.81	**0.969**	0.907	0.965
$\sigma = 20$	**25.46**	23.11	25.26	0.936	0.902	**0.937**
$\sigma = 30$	**23.22**	21.43	23.17	0.904	0.866	**0.908**
$\sigma = 40$	21.71	20.29	**21.73**	0.871	0.833	**0.878**
$\sigma = 50$	20.50	19.26	**20.59**	0.837	0.797	**0.849**
Fig. 5	PSNR			SSIM		
$\sigma = 10$	24.04	25.70	**27.51**	0.651	0.771	**0.847**
$\sigma = 20$	23.18	23.57	**24.51**	0.605	0.666	**0.728**
$\sigma = 30$	22.28	22.32	**22.89**	0.539	0.571	**0.623**
$\sigma = 40$	21.48	21.49	**21.97**	0.461	0.495	**0.553**
$\sigma = 50$	20.97	20.91	**21.25**	0.409	0.440	**0.490**

polyphase order was set to $N_{\mathrm{y}} = N_{\mathrm{x}} = 4$ for the DirLOTs. Since the basis size is $L_{\mathrm{y}} \times L_{\mathrm{x}} = 10 \times 10$ in this case, Symlet of index 5 was used as a reference of separable orthonormal DWT, where the support size is identical to the adopted DirLOTs. The number of levels for constructing DWTs is selected as three. The variance σ^2 was estimated by applying the robust median estimator to the finest wavelet coefficients.

By observing Figs. 4 and 5, the DirLOT with the TVMs shows better quality for diagonal edges compared with the results of Sym5 and VM2 [17]. Table I compares the denoising performances among three transforms for various noise levels. In the table, the DirLOT with TVMs shows almost the best performance among the three transforms, especially in terms of the structural similarity (SSIM) index [18]. This means that the DirLOTs with the TVMs represent the diagonal structure appropriately and yield perceptually pleasant results.

V. CONCLUSIONS

This paper proposed to adopt the hierarchical tree construction of DirLOTs to image denoising. The SURE-LET approach was firstly reviewed as the orthonormal wavelet-based denoising technique. Since the conventional separable transform has the disadvantage that the bases are not simultaneously allowed to be anisotropic with the fixed-critically-subsampling, overlapping, orthogonal, symmetric, real-valued and compact-support property, the SURE-LET approach remains room to improve the performance for diagonal textures and edges. From some experimental results, it was shown that the combination of the SURE-LET approach as the shrinkage function and a hierarchical DirLOT as the DWT overcomes the geometric problem.

ACKNOWLEDGMENT

This work was supported by JSPS KAKENHI (23560443).

REFERENCES

[1] M. Elad, "Why simple shrinkage is still relevant for redundant representations?" *IEEE Trans. Inf. Theory*, vol. 52, no. 12, pp. 5559–5569, Dec. 2006.

[2] D. L. Donoho and I. M. Johnstone, "Ideal spatial adaptation by wavelet shrinkage," *Biometrika*, vol. 81, no. 3, pp. 425–455, 1994.

[3] ——, "Adapting to unknown smoothness by wavelet shrinkage," *J. Amer. Statist. Assoc.*, vol. 90, no. 432, pp. 1200–1224, Dec. 1995.

[4] F. Luisier, T. Blue, and M. Unser, "A new SURE approach to image denoising: Interscale orthonormal wavelet thresholding," *IEEE Trans. Image Process.*, vol. 16, no. 3, pp. 593–606, Mar. 2007.

[5] T. Blu and F. Luisier, "The SURE-LET approach to image denoising," *IEEE Trans. Image Process.*, vol. 16, no. 11, pp. 2778–2786, Nov. 2007.

[6] F. Luisier and T. Blu, "SURE-LET multichannel image denoising: Interscale orthonormal wavelet thresholding," *IEEE Trans. Image Process.*, vol. 17, no. 4, pp. 482–492, Apr. 2008.

[7] S. Mallat, *A Wavelet Tour of Signal Processing, Third Edition: The Sparse Way*. Academic Press, 2008.

[8] J. Ma and G. Plonka, "The curvlet transform - a review of recent applications," *IEEE Signal Process. Mag.*, vol. 27, no. 2, pp. 118–133, Mar. 2010.

[9] J.-L. Starck, F. Murtagh, and J. M. Fadili, *Sparse Image and Signal Processing: Wavelets, Curvelets, Morphological Diversity*. Cambridge University Press, 2010.

[10] M. Vetterli, "Wavelets, approximation, and compression," *IEEE Signal Process. Mag.*, pp. 59–73, Sep. 2001.

[11] M. N. Do and M. Vetterli, "The contourlet transform: An efficient directional multiresolution image representation," *IEEE Trans. Image Process.*, vol. 14, no. 12, pp. 2091–2106, Dec. 2005.

[12] A. L. da Cunha and M. N. Do, "On two-channel filter banks with directional vanishing moments," *IEEE Trans. Image Process.*, vol. 16, no. 5, May 2007.

[13] S. Muramatsu and M. Hiki, "Block-wise imprementation of directional GenLOT," in *IEEE Proc. of ICIP*, Nov. 2009, pp. 3977–3980.

[14] T. Kobayashi, S. Muramatsu, and H. Kikuchi, "2-D nonseparable GenLOT with trend vanishing moments," in *IEEE Proc. of ICIP*, Sep. 2010, pp. 385–388.

[15] S. Muramatsu, D. Han, T. Kobayashi, and H. Kikuchi, "Theoretical analysis of trend vanishing moments for directional orthogonal transforms," in *Proc. of Picture Coding Symp.*, Dec. 2010, pp. 130–133.

[16] S. Muramatsu, T. Kobayashi, D. Han, and H. Kikuchi, "Design method of directional GenLOT with trend vanishing moments," in *Proc. of APSIPA ASC*, Dec. 2010, pp. 692–701.

[17] A. Adachi, S. Muramatsu, and H. Kikuchi, "Constraints of second-order vanishing moments on lattice structures for non-separable orthogonal symmetric wavelets," *IEICE Trans. Fundamentals*, vol. E92-A, no. 3, pp. 788–797, Mar. 2009.

[18] Z. Wang, A. C. Bovik, H. R. Sheikh, and E. P. Simoncelli, "Image quality assessment: From error visibility to structural similarity," *IEEE Trans. Image Process.*, vol. 13, no. 4, pp. 600–612, Apr. 2004.